International Journal of Nanomedicine

Dovepress
Taylor & Francis Group

Open Access Full Text Article

ORIGINAL RESEARCH

Amphiphilic Chitosan–PEI Hybrid Nanocarrier Enhances Delivery Efficiency and Immunogenicity of PEDV mRNA Vaccines

Shangen Xu[1–4], Haiwen Zhong[1], Linyun Li[1], Yao Chen[1], Chenxi Sun[1], Zhicheng Lao[1], Afei Wang[1], Tianyu Qian[1], Xiaohua Wang[1–4], Kai Zhao[1–4]

[1]Zhejiang Key Laboratory for Restoration of Damaged Coastal Ecosystems, School of Life Sciences, Taizhou University, Taizhou, Zhejiang, 318000, People's Republic of China; [2]Zhejiang International Science and Technology Cooperation Base for Biomass Resources Development and Utilization, School of Life Sciences, Taizhou University, Taizhou, Zhejiang, 318000, People's Republic of China; [3]Taizhou Key Laboratory of Biomedicine and Advanced Dosage Forms, School of Life Sciences, Taizhou University, Taizhou, Zhejiang, 318000, People's Republic of China; [4]Zhejiang-Malaysia Joint Laboratory for Bioactive Materials and Applied Microbiology, School of Life Sciences, Taizhou University, Taizhou, Zhejiang, 318000, People's Republic of China

Correspondence: Kai Zhao, Email zybin395@126.com

Background: mRNA vaccines require efficient and safe delivery systems to achieve robust antigen expression and immune activation. Chitosan is widely recognized for its biocompatibility and adjuvant properties; however, its application in mRNA delivery remains underexplored. This study aimed to develop a chitosan-derived nanoparticle system capable of enhancing mRNA transfection efficiency and vaccine immunogenicity.

Methods: A novel chitosan derivative, PAN2H, was synthesized by grafting palmitic acid (PA) onto N-2-hydroxypropyl trimethyl ammonium chloride chitosan (N-2-HACC). mRNA-loaded nanoparticles (PEI/mRNA/PAN2H) were constructed by first complexing mRNA with polyethyleneimine (PEI) and subsequently electrostatically binding the complex to PAN2H. Transfection efficiency was evaluated using GFP- and Luc-mRNA. Porcine epidemic diarrhea virus (PEDV) S1- and RBD-mRNA were selected as vaccine antigens for in vivo immunization to assess cellular and humoral immune responses.

Results: Compared with PEI-mediated transfection, PEI/mRNA/PAN2H nanoparticles achieved approximately twofold higher expression of GFP- and Luc-mRNA in vitro, indicating that PAN2H incorporation markedly enhances mRNA transfection. In vivo, PEI/mRNA/PAN2H vaccination elicited significantly stronger antibody responses and cellular immune activation than the PEI control, supporting improved antigen expression and immune stimulation. Importantly, the PAN2H–PEI hybrid strategy provides a practical way to enhance PEI-based delivery by combining electrostatic condensation (PEI) with amphiphilicity-driven assembly and chitosan-associated biocompatibility/adjuvanticity (PAN2H).

Conclusion: The cationic PEI/mRNA/PAN2H nanoparticles exhibit low cytotoxicity and markedly improved mRNA delivery capabilities. These findings highlight PAN2H as a promising chitosan-derived platform for developing next-generation mRNA vaccines.

Keywords: chitosan-based nanomaterials, PAN2H, mRNA delivery system, polyethylenimine, vaccine

Introduction

In recent years, substantial research investment and technological breakthroughs have made mRNA a promising platform for vaccine development. Notably, the FDA-approved COVID-19 mRNA vaccines have demonstrated the tremendous potential of mRNA technology in preventing SARS-CoV-2 infections.[1,2] As the main component of mRNA vaccines, the delivery system plays a crucial role, and lipids are the most widely used and much attention has been given to developing lipid-based mRNA delivery nanotechnologies.[3] However, little attention has been paid to other material types, particularly polymer-based nanomaterials. Non-lipid polymeric carriers offer complementary advantages such as modular

https://doi.org/10.2147/IJN.S514056
Received: 18 December 2025
Accepted: 13 March 2026
Published: 17 March 2026

Graphical Abstract

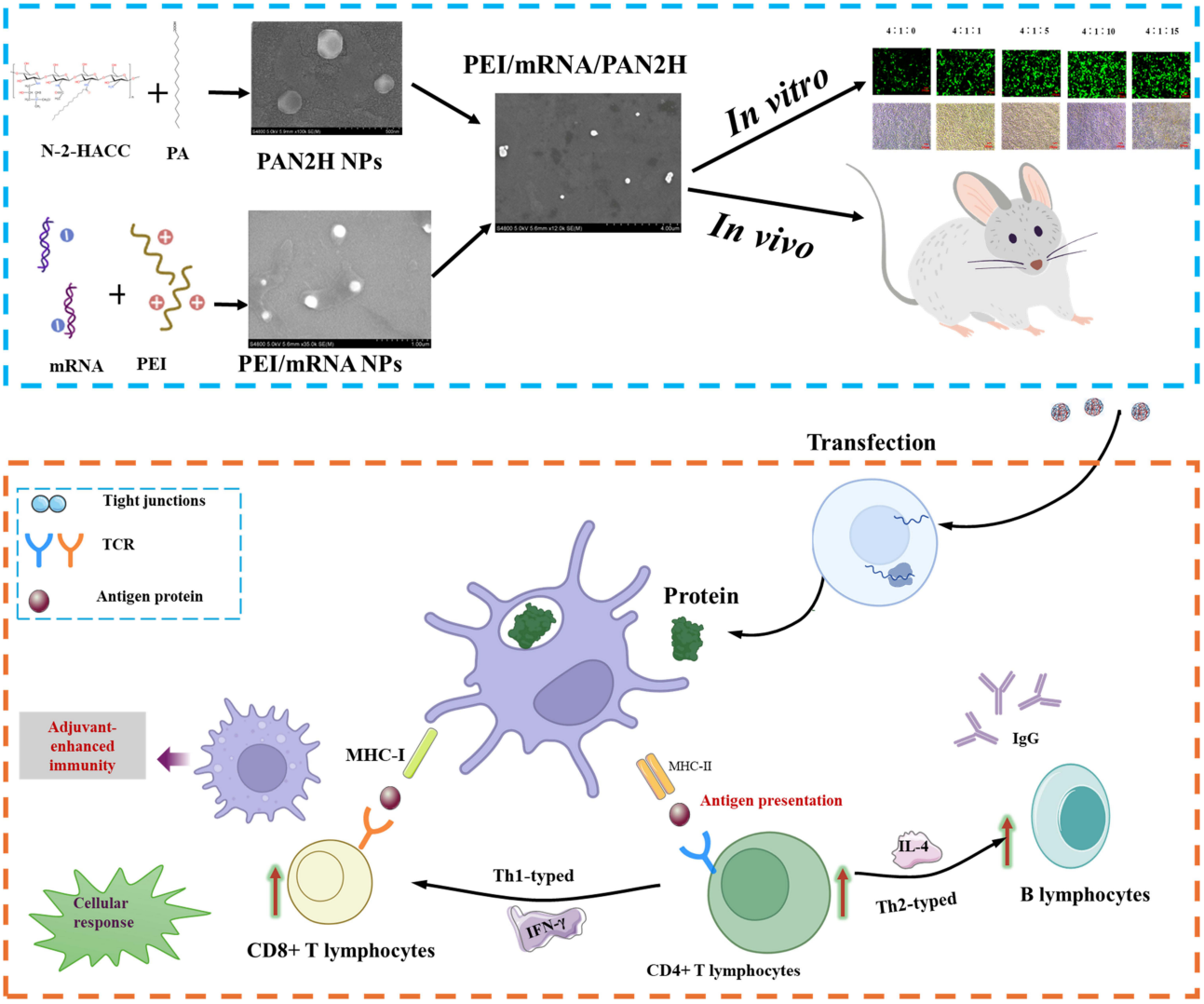

chemistry, scalable preparation, and tunable interactions with biological barriers, but they still face major challenges in mRNA stabilization, serum tolerance, cellular uptake, and endosomal escape compared with LNPs.

Chitosan is a good polymeric gene carrier due to its ability to load large amounts of nucleic acids and its good biocompatibility. However, chitosan's poor solubility under physiological conditions, poor buffering capacity, and insufficient targeting ability limit its further application in gene delivery.[4] In order to solve the shortcomings of low water solubility of chitosan, researchers have synthesized a variety of chitosan derivatives by quaternization, carboxymethylation and graft copolymerization of the active amino and hydroxyl groups of chitosan with various chemical modifications, which effectively improve the water solubility, specific targeting and gene release efficiency of chitosan.[5–12] Currently, chitosan and its derivatives have been extensively studied in gene delivery systems, mainly for delivering miRNA, pDNA and siRNA, and have yielded satisfactory treatment results in a variety of diseases, but its application in mRNA vaccine delivery remains limited and is far less explored than its use for pDNA/siRNA delivery.[13,14] This gap is

important since mRNA differs from pDNA/siRNA in size and structural flexibility, and it requires efficient cytosolic release for translation, making carrier design and stability in biological media particularly critical.[15,16]

Polyethylenimine (PEI) is a cationic polymer commonly used as a gene delivery vector material, capable of condensing nucleic acids into nanoscale structures through electrostatic interactions.[17] PEI possesses a high cationic charge density, and its amino groups exhibit a large buffering capacity at physiological pH, contributing to the complex's lysosomal escape. However, despite its high transfection effect, its poor biodegradability and high charge density can cause damage to cell membranes. To overcome the problem of PEI toxicity, researchers have proposed several approaches. One approach is to introduce biodegradable linkers to generate degradable PEI-based carriers, and another widely used approach is to shield excessive cationic charges by association with biocompatible polysaccharides. To date, PEI has been used in combination with a variety of biodegradable and biocompatible compounds including chitosan, O-carboxymethyl chitosan dextran, N-octyl-N-quaternary chitosan, vitamin E succinate, starch and cyclodextrins.[16,18–24] There are also other approaches in which nanoparticles are coated or associated with PEI, and this can significantly improve the transfection efficiency and reduce the PEI cytotoxicity.[25] Currently, many reports have been published on the use of chitosan coupled with PEI to deliver DNA and siRNA, but few studies have examined its delivery of mRNA.[19,26,27] Considering the importance of mRNA vaccines, it is of great significance to develop chitosan-PEI mRNA delivery system vaccines. However, most reported chitosan–PEI assemblies are predominantly electrostatic, which may still suffer from limited membrane interaction and reduced performance under serum-containing conditions—issues that are particularly relevant for mRNA delivery.[16]

Porcine epidemic diarrhea virus (PEDV or PED virus) is a re-endemic coronavirus that infects pigs of all ages and causes severe intestinal disease, with dehydration and diarrhea in infected pigs, especially with mortality rates of up to 100% in newborn piglets aged 1–7 days.[28,29] However, due to the high variability of PEDV, most of the current commercial attenuated and inactivated vaccines are unable to effectively control PEDV infection, and traditional vaccines suffer from long preparation period, weak immunization effect and limited safety profiles. Therefore, the development of a new mRNA vaccine with simple preparation, good immunization effect and high safety is of great significance for the prevention and control of PEDV. Studies have shown that neutralizing antibodies induced by the RBD region of the PEDV S protein effectively neutralize PEDV and are the main choice for novel subunit vaccines.[30–32] In this study, we report a chitosan-PEI-based mRNA delivery strategy that enhances the transfection efficiency and immunogenicity of mRNA vaccines. First, we synthesized the nucleic acid delivery nanocarrier PAN2H. The amphiphilic design rationale of PAN2H is that grafting palmitic acid onto quaternized chitosan introduces a hydrophobic segment that can promote self-assembly and strengthen membrane interactions, while the quaternary ammonium groups maintain water solubility and provide stable electrostatic association with nucleic acids. Amphiphilic chitosan systems have been reported to form nanomicelles and enhance nonviral gene delivery by combining electrostatic complexation with hydrophobic assembly.[33,34] Subsequently, we screened the optimal ratio of PEI/mRNA/PAN2H, and the in vitro experiments indicated that PEI/mRNA/PAN2H could effectively enhance the mRNA transfection efficiency and protect from nuclease degradation. Compared with conventional chitosan–PEI systems or other non-lipid polymeric carriers, the PAN2H–PEI hybrid strategy is intended to integrate PEI-driven condensation/endosomal buffering with amphiphilicity-assisted assembly and membrane interaction, thereby improving delivery efficiency while potentially reducing the PEI burden.[19,27] The results showed that the mRNA nanovaccine encapsulating PEI/mRNA/PAN2H could improve the low expression and sub-optimal safety profile associated with the PEI delivery system and enhance its immunization effect, which provided a technical reserve for the further development of mRNA vaccines.

Materials and Methods

Materials and Chemicals

Branched poly(ethyleneimine) (PEI; Sigma-Aldrich, USA; cat. no. 408727; average Mw ~25,000; average Mn ~10,000 by GPC) was used as the cationic condensing agent. Palmitic acid (PA), 1-ethyl-3-(3-dimethylaminopropyl)carbodiimide hydrochloride (EDC), and N-hydroxysuccinimide (NHS) were used for PAN2H synthesis. *RNase* I was obtained from Thermo Fisher Scientific (cat. no. EN0601; 10 U/μL). Cell Counting Kit-8 (CCK-8) was purchased from Beyotime,

China. HEK-293T (ATCC CRL-3216), Vero (ATCC CCL-81), L929 (ATCC CCL-1), and 4T1 (ATCC CRL-2539) cells were obtained from ATCC (Manassas, VA, USA). The dendritic cell line DC2.4 was obtained from Merck (Rahway, NJ, USA). Anti-mouse PE-CD8 and anti-mouse PE/Cy7-CD4 antibodies were purchased from BioLegend (USA). Unless otherwise indicated, all other reagents were of analytical grade.

Animals and Ethics Statement

Six- to eight-week-old specific pathogen-free (SPF) BALB/c mice were purchased from Hangzhou Qizhen Technology Co., Ltd. (License No.: SCXK (Zhe) 2022-0005). All animal experiments were conducted at the Laboratory Animal Center of Taizhou University and were approved by the Laboratory Animal Welfare and Ethics Committee of Taizhou University (Ethics approval number: TZXY-2022-20221034).

All procedures involving animals were performed in strict accordance with the Guide for the Care and Use of Laboratory Animals issued by the National Research Council and complied with internationally accepted ethical standards for animal research. For sample collection and terminal procedures, mice were humanely euthanized under deep anesthesia. Briefly, animals were anesthetized using isoflurane inhalation until complete loss of reflexes was confirmed, followed by cervical dislocation as a secondary physical method to ensure death. All euthanasia procedures were performed in accordance with the American Veterinary Medical Association (AVMA) Guidelines for the Euthanasia of Animals. Every effort was made to minimize animal suffering and to reduce the number of animals used.

mRNA Preparation and Modification

The mRNAs used in this study were generated by in vitro transcription using a T7 promoter–based transcription kit (Novoprotein, China, E131). During transcription, N1-Methyl-Pseudo-UTP was incorporated in place of uridine to enhance mRNA stability and translational performance. Following transcription, the mRNA products were subjected to cap addition using a capping reaction kit (Novoprotein, China, M082) in accordance with the manufacturer's protocol. The capped mRNAs were subsequently purified, quantified, and stored under *RNase*-free conditions until further use. Unless otherwise indicated, all mRNA preparations used in this study were produced using this same procedure.

PAN2H Synthesis and Characterization

PA-N-2-HACC(PAN2H) was synthesized according to our previous protocols.[35] Briefly, N-2-HACC (0.30 g; substitution degree 37.5%, prepared in-house as previously reported) was dissolved in distilled water (40 mL) in a 250 mL two-neck round-bottom flask. In parallel, PA (0.26 g) was dissolved in dichloromethane (20 mL), followed by the addition of EDC (0.22 g) and NHS (0.14 g). The mixture was stirred at 40 °C for 2 h to activate PA. The organic solvent was then removed by evaporation to obtain the EDC-activated PA, which was subsequently re-dissolved in anhydrous ethanol (20 mL). Under 70 °C water-bath stirring, the activated PA solution in ethanol was added dropwise to the aqueous N-2-HACC solution and allowed to react for 24 h. After completion, the reaction mixture was purified by dialysis against 30% (v/v) ethanol followed by dialysis against distilled water. The final product was obtained by lyophilization to yield PAN2H (approximately 0.20 g of lyophilized PAN2H was obtained). To demonstrate the successful synthesis of PAN2H, the structures of the synthesized N-2-HACC and PAN2H were assayed by using NMR spectroscopy (Bruker, AVANCE III HD 400, Germany). The palmitic-acid grafting degree of substitution (DS_PA) of PAN2H was quantified from the ^{1}H NMR spectra, where the characteristic signals at $\delta = 0.88$ ppm and $\delta = 1.24$ ppm were assigned to the terminal methyl (-CH3) and methylene (-CH2-) protons of the grafted PA chains, respectively. Based on the NMR integration, the degree of substitution (DS) of PA was determined to be 10.35%.

Determination of CMC by Conductivity

The critical micelle concentration (CMC) of PAN2H was determined by conductivity measurements. A series of PAN2H solutions with different concentrations were prepared in deionized water (no added salt) to cover the concentration range below and above the expected CMC. Conductivity was measured at 25 °C. For baseline correction, the conductivity of deionized water was measured under identical conditions and subtracted from each sample value to obtain blank-corrected specific conductivity. The blank-corrected specific conductivity was plotted against logC, which exhibited

two distinct linear regimes. The CMC was determined as the breakpoint defined by the intersection of two linear regressions fitted to the low- and high-concentration regions (piecewise linear fitting). Using this method, the CMC of PAN2H was 0.085 mg/mL; above this concentration, PAN2H self-assembled into micelles in aqueous solution and could be further processed by ultrasonication to form nanoparticles. The hydrophobic palmitoyl chain substitution likely promotes self-aggregation by enhancing hydrophobic interactions, thereby facilitating the formation of compact polymer aggregates.

Production of Optimal PEI/mRNA/PAN2H NPs

In brief, PEI/mRNA/PAN2H nanoparticles were prepared by stepwise electrostatic assembly. Branched poly-(ethyleneimine) (PEI; Sigma-Aldrich, USA; cat. no. 408727; average Mw ~25,000 by light scattering; average Mn ~10,000 by GPC) was first mixed with mRNA at the indicated amount, vortexed for 30s, and allowed to stand for 5 min to form PEI/mRNA complexes. Subsequently, PAN2H (50 mg) was dissolved in *RNase*-free water (50 mL) and pre-dispersed by ultrasonication using a probe-type ultrasonic cell disruptor (FS-1800N, Shanghai Sonxi Ultrasonic Instrument Co., Ltd., China; 20 kHz) at an output power of 90 W for 10 min (continuous mode, 100% duty cycle) to obtain a homogeneous PA–N-2-HACC dispersion. The sonication was performed in an ice-water bath to minimize heating; the probe tip diameter was 20 mm. Then, the ultrasonication-treated PAN2H was added, followed by vortexing for 30s and incubation for 10 min to obtain the PEI/mRNA/PAN2H nanoparticles.

Characterization of the PEI/mRNA/PAN2H NPs

Nanoparticle morphology was examined by scanning electron microscopy (SEM). Briefly, 10 μL of nanoparticle dispersion in water was dropped onto a silicon wafer and allowed to air-dry at room temperature. The dried samples were gold-sputtered under vacuum for 30s and imaged using a field-emission SEM (S-4800; Hitachi, Japan) at an accelerating voltage of 20 kV. The magnification used was 35,000× for PAN2H nanoparticles and 110,000× for PEI/mRNA/PAN2H nanoparticles. Zeta Sizer ZS90 (Malvern Instruments Ltd., Southborough, MA, USA) was used to assay the zeta potential and particle size of PEI/mRNA/PAN2H NPs.

The Stability of the PEI/mRNA/PAN2H NPs

An *RNase* protection assay was performed to evaluate whether PEI/PAN2H nanoparticles protect mRNA from nuclease degradation. Briefly, Naked mRNA and mRNA-loaded nanoparticles were each prepared to contain 1 μg mRNA per reaction. *RNase* I (Thermo Fisher Scientific, catalog no. EN0601; 10 U/μL) was added (1 μL per reaction) and samples were incubated at 37 °C for 30 min. The reaction was terminated by adding 10× denaturing loading buffer followed by heat denaturation (95 °C for 5 min) prior to agarose gel electrophoresis to assess RNA integrity.

CCK-8 Cytotoxicity Assay

Cell viability was evaluated using a CCK-8 assay. Cells were seeded in 96-well plates and treated with PAN2H, PEI, or PEI/PAN2H formulations at the indicated concentrations for 24 h. All doses are reported as mass concentrations (μg/mL). For PEI/PAN2H nanoparticles, the reported dose represents the total carrier concentration (PEI + PAN2H, μg/mL) in the formulation at the fixed mass ratio used. For nanoparticle-treated groups, the mRNA dose was maintained at a constant concentration of 1 μg/mL. After incubation, CCK-8 reagent was added and absorbance was measured to calculate cell viability, which was normalized to untreated controls.

In vitro Transfection of the PEI/mRNA/PAN2H NPs

The delivery efficacy of EGFP- and Fluc-mRNA by PEI/PAN2H NPs were then evaluated. Briefly, HEK-293T cells were digested and plated at a density of 5×10^4 per well in 24-well plates and then cultured for 24 hours before transfection. Then, the 1 μg mRNA was mixed with PEI at a mass ratio of 4:1 for 5 min, and mixed with nanoparticles PAN2H at different mass ratios (4:1:1, 4:1:5, 4:1:10, 4:1:15), vortexed for 30s after mixing, and left to stand at 25°C for 10 min to form the PEI/mRNA/PAN2H NPs. Next, the prepared mRNA nanoparticles were slowly added to the HEK-293T cells

and then incubated for another 28 hours. Subsequently, cells were harvested and the expression of eGFP and Fluc proteins was determined by immunofluorescence and firefly luciferase assays.

Immunization with the PEI/mRNA/PAN2H NPs

Forty-two 6–8-week-old SPF BALB/c mice were randomized into seven groups (n = 6 per group). Group 1–7 received PBS, PEI, PAN2H, PEI/RBD (30 μg RBD mRNA), PEI/S1 (30 μg S1 mRNA), PEI/RBD/PAN2H (30 μg RBD mRNA), and PEI/S1/PAN2H (30 μg S1 mRNA), respectively. Immunizations were administered by intramuscular (i.m.) injection. The prime vaccination was performed at Day 0, followed by a booster at Day 14.

Randomization was performed using simple random allocation after confirmation of normal activity and body weight. Investigators conducting ELISA, flow cytometry, and data analysis were blinded to group allocation. All mice were housed under identical conditions and handled according to the same experimental schedule. Inclusion criteria required healthy animals without clinical abnormalities at baseline. Predefined exclusion criteria included non-treatment-related illness, accidental injury, technical dosing failure, or compromised biological samples; no exclusions occurred during the study.

Detection of IgG Antibody, IL-4, and IFN-γ

To evaluate vaccine-induced humoral and cellular immune responses, serum samples were collected from all immunized mice at weeks 2, 4, and 6 after the prime immunization (Day 0). PEDV-specific antibody responses were determined by ELISA. Briefly, 96-well plates were coated with recombinant full-length PEDV S protein (10 ng per well in 0.1 mL) and incubated at 4 °C overnight. After blocking, serially diluted mouse sera were added, and bound antibodies were detected following standard ELISA procedures. The levels of total mouse IgG, IgG1, and IgG2a were quantified using commercial ELISA kits (eBioscience, USA) according to the manufacturers' instructions. Because RBD and S1 are domains of the PEDV S protein, this assay reflects S-binding antibody responses, including antibodies elicited by RBD- or S1-encoding mRNA vaccines. For cytokine analysis, sera collected at weeks 2, 4, and 6 were used to measure IL-4 and IFN-γ levels using mouse IL-4 and IFN-γ ELISA kits (eBioscience, USA) following the manufacturers' protocols.

Flow Cytometry Analysis and Lymphocyte Proliferation Measurements

To evaluate lymphocyte proliferation after immunization, splenocytes were isolated from mouse spleens at the indicated time point and the stimulation index (SI) was determined using a CCK-8 assay (Beyondi, China). Briefly, splenocytes were adjusted to the required density and plated in 96-well plates with appropriate stimulation and control conditions (each sample in technical replicates), followed by CCK-8 incubation and absorbance measurement according to the manufacturer's instructions; SI was calculated as the ratio of stimulated to control wells.[36]

Flow cytometry was performed to quantify $CD4^+$ and $CD8^+$ T-cell populations in mouse spleens after immunization. At the indicated time point, spleens were collected aseptically and processed into single-cell suspensions. After removal of debris and erythrocyte contamination as appropriate, the cells were resuspended in staining buffer and incubated with anti-mouse PE-CD8 and anti-mouse PE/Cy7-CD4 antibodies (BioLegend, USA) for 30 min at 4 °C in the dark. After staining, the cells were washed twice with PBS and analyzed using a BD FACSVerse flow cytometer (BD Biosciences, USA). During data analysis, lymphocyte events were identified according to forward- and side-scatter characteristics to exclude debris and non-lymphocyte populations. Events with abnormal scatter characteristics and cell aggregates were further excluded to improve data quality. Fluorescence compensation was performed using single-stained controls before sample acquisition, and the same analysis settings and quadrant criteria were applied consistently across all samples. $CD4^+$ and $CD8^+$ T-cell subsets were quantified on CD4 (PE/Cy7) versus CD8 (PE) dot plots.

Statistical Analysis

Data is presented as mean ± SD. For animal experiments, n = 6 mice per group unless otherwise specified. For serum ELISA, cytokine, splenocyte proliferation, and flow-cytometry analyses, n refers to the number of mice actually analyzed per group. Unless otherwise indicated, these assays were performed using samples from 3 mice per group. Statistical comparisons among multiple groups were performed using one-way ANOVA, followed by Tukey's post hoc multiple-

comparisons test where appropriate. For experiments involving two independent variables, two-way ANOVA with an appropriate multiple-comparisons adjustment was applied. Prior to ANOVA, the assumptions of normality and homogeneity of variance were evaluated; when these assumptions were not met, a suitable non-parametric alternative was used. Exact p values were reported where feasible, and $p < 0.05$ was considered statistically significant. Statistical significance was defined as follows: $p < 0.05$ (*), $p < 0.01$ (**), $p < 0.001$ (***), and $p < 0.0001$ (****); ns indicates no significant difference. Statistical analyses were performed using GraphPad Prism 8 software.

Results

Preparation of the PEI/mRNA/PAN2H NPs

PAN2H was prepared by grafting the hydrophobic chain segment PA onto N-2-HACC via EDC/NHS amide condensation reaction (Figure 1A). The success of the synthesis was confirmed by ^{1}H NMR spectroscopy (Figure 1B), where the characteristic signals at δ = 0.88 ppm and δ = 1.24 ppm were assigned to the terminal methyl (-CH3) and methylene (-CH2-) protons of the grafted PA chains, respectively. Based on the NMR integration, the degree of substitution (DS) of PA was determined to be 10.35%. Then, the critical micelle concentration of PAN2H was measured by conductivity. The results indicated that the CMC value of PAN2H was 0.085 mg/mL, and when the concentration of PAN2H in aqueous solution exceeded 0.085 mg/mL, PAN2H micelles were formed, and nanoparticles were formed after sonication (Figure 1C).

SEM observation showed that PAN2H nanoparticles exhibited a roughly spherical morphology (Figure 2A). The zeta potentials of PAN2H NPs, PEI, and naked mRNA were 53.7 ± 3.2 mV, 19.2 ± 2.5 mV, and −55.8 ± 2.7 mV, respectively

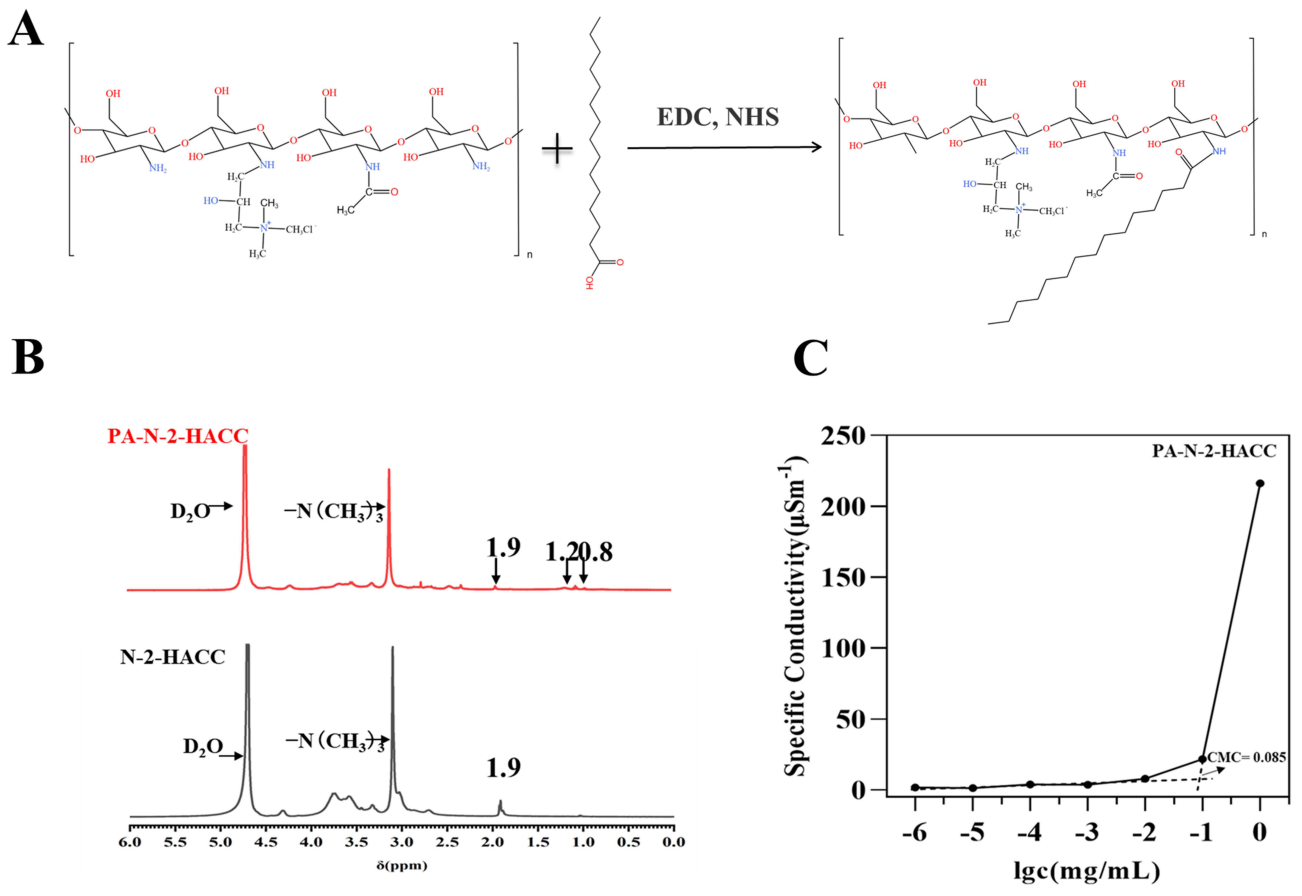

Figure 1 Preparation of the PAN2H NPs. (**A**) Schematic illustration of the EDC/NHS-mediated conjugation used to synthesize PAN2H from N-2-HACC and the hydrophobic moiety. (**B**) ^{1}H NMR spectra recorded in D2O: the upper spectrum corresponds to PAN2H and the lower spectrum corresponds to N-2-HACC; characteristic signals are annotated in the spectra. (**C**) Specific conductivity as a function of concentration (logC) for PAN2H, showing the critical micelle concentration (CMC = 0.085 mg/mL).

https://doi.org/10.2147/IJN.S514056

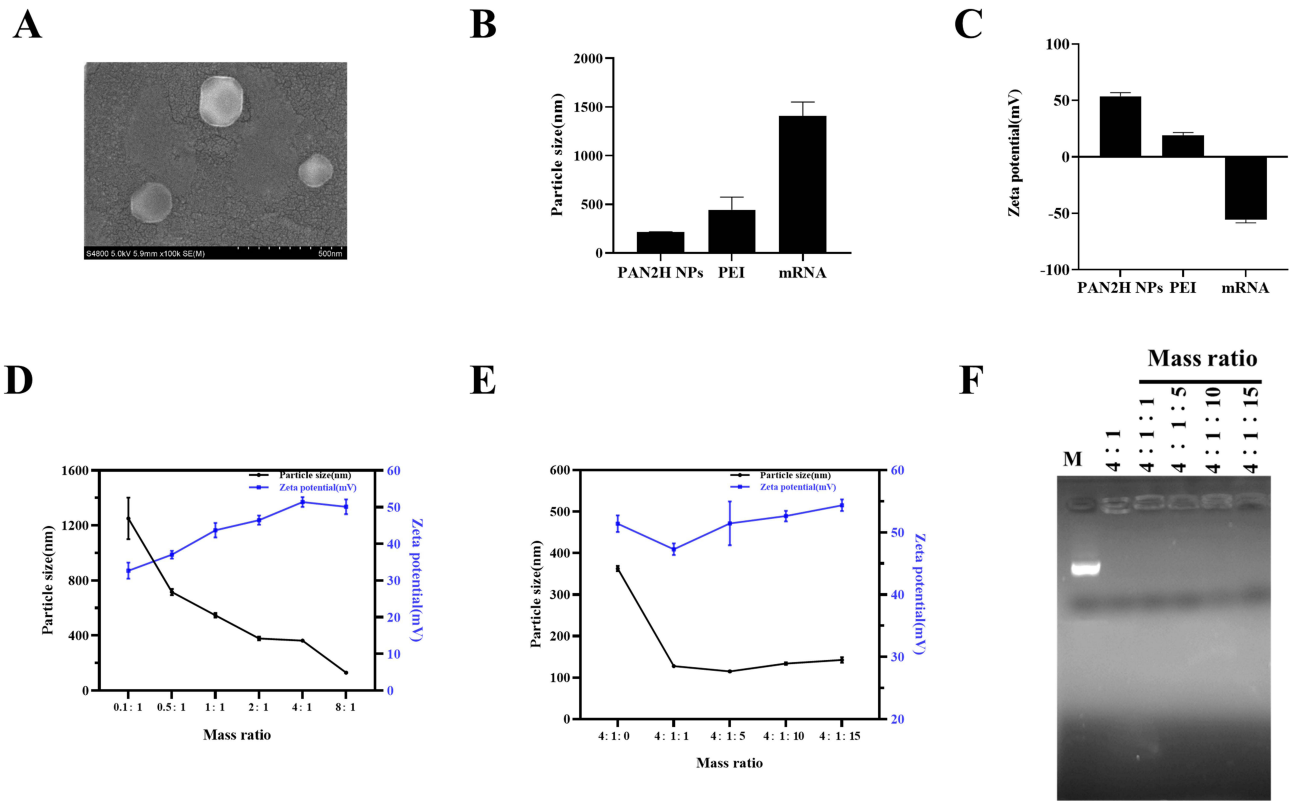

Figure 2 Preparation of the PEI/mRNA/PAN2H NPs. (**A**) SEM scanning morphology of PAN2H NPs; (**B**) Average particle size of PAN2H, PEI, and naked mRNA; (**C**) Zeta potential of PAN2H, PEI, and naked mRNA; (**D**) Particle size and zeta potential of PEI:mRNA complexes at different mass ratios; (**E**) Particle size and zeta potential of PEI: mRNA:PAN2H complexes at different mass ratios. (**F**) T Agarose gel retardation assay of PEI:mRNA:PAN2H complexes.

(n = 3, mean ± SD, Table S1). The average particle sizes of PAN2H, PEI, and mRNA were 213.4 nm, 442.5 nm, and 1413.3nm, respectively (n = 3) (Figure 2B and C).To prepare the mRNA delivery system, the effects of concentration on the particle size and zeta potential were detected by adjusting the mass ratios of different PEI, PAN2H, and mRNA. As shown in Figure 2D, increasing the PEI mass ratio decreased particle size and increased zeta potential, supporting effective PEI-mediated condensation of mRNA. Similarly, as the amount of PAN2H incorporated into the PEI/mRNA complexes increased, both particle size and zeta potential increased (Figure 2E). To further evaluate mRNA binding to PEI or PEI/PAN2H, formulations were prepared at defined mass ratios (w/w, μg:μg) and assessed by agarose gel retardation. As shown in Figure 2F, complete retardation was achieved when PAN2H was incorporated into PEI/mRNA complexes, as evidenced by no detectable migrating free mRNA band. The binding threshold was observed starting from a mass ratio (w/w, μg:μg:μg) of PEI:mRNA:PAN2H = 4:1:1. To investigate further the mechanism of nanoparticle assembly, a heparin competition assay was performed. As shown in Figure S1, a concentration-dependent reappearance of free mRNA bands was observed upon heparin treatment, indicating effective competitive displacement of mRNA from the nanoparticles. Taken together, these results confirm that electrostatic interactions play a dominant role in stabilizing the mRNA–polymer complexes.

In vitro Safety and Transfection Assay of the PEI/mRNA/PAN2H NPs

The appropriate dose of carrier material was determined by CCK-8 assay. As shown in Figure 3A, cell survival was higher than 80% when the concentrations of PAN2H and PEI were 50 μg/mL, and lower than 80% when the concentrations were 100 μg/mL. Compared with PAN2H and PEI, the toxicity of PEI/PAN2H showed a decreasing trend, and the cell viability was still higher than 80% when the concentrations were 100 μg/mL.

To screen the optimal ratio of PEI:PAN2H, eGFP- and Fluc- mRNA were selected as the mRNA models, and the mass ratio of PEI to mRNA was fixed at 4:1 (w/w) according to the recommended ratio, and then PAN2H with mass ratios of

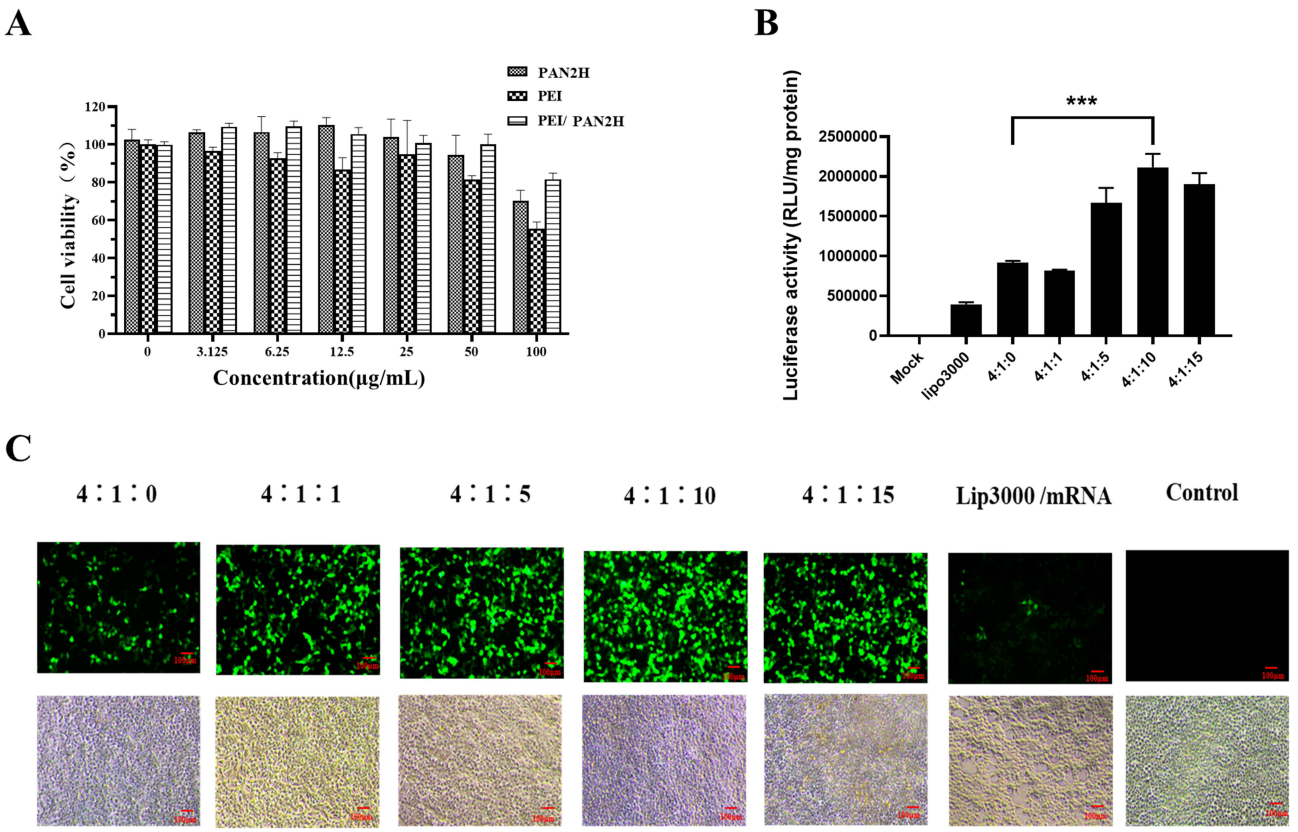

Figure 3 Evaluation of the in vitro safety and transfection efficiency of the PEI/mRNA/PAN2H NPs. (**A**) Evaluation of in vitro safety of PAN2H, PEI, and PEI/mRNA/PAN2H NPs; (**B**) Identification of in vitro transfection experiments with different mass ratios of PEI, PEI/PAN2H, and Fluc mRNA; (**C**) Identification of in vitro transfection experiments with different mass ratios of PEI, PEI/PAN2H, and eGFP mRNA. Data are presented as mean ± SD (n = 3). Statistical significance: ***$p < 0.001$.

1, 5, 10, and 15 μg/mL were added, the commercial transfection reagent PEI and Lipofectamine 3000 (Lipo3000) were used as positive control. The ratios with appropriate cell transfection efficiency were screened by inverted fluorescence microscopy and Fluc assay. As shown in Figure 3B and C, luciferase expression differed significantly across PAN2H ratios (n = 3, mean ± SD). The 4:1:10 formulation yielded the highest mean luciferase activity, which was significantly higher than 4:1:5 ($p = 0.0118$) and higher than 4:1:0 and 4:1:1 ($p < 0.0001$ for both) by Tukey's multiple-comparisons test, while it was not significantly different from 4:1:15 ($p = 0.3349$). Consistently, the strongest green fluorescence signals were observed at PEI/mRNA/PAN2H = 4:1:10 (Figure 3C). Overall, in the presence of serum (2% FBS, v/v), the transfection efficiency of the PEI/mRNA/PAN2H group was superior to that of the commercial reagents PEI and Lipo3000, suggesting that the addition of PAN2H within a certain range can improve the transfection efficiency of mRNA. Subsequently, we evaluated the transfection ability of PEI/mRNA/PAN2H in different cells (L929 cells, 293T cells, DC2.4 cells, 4T1 cells, Vero cells), as shown in Figure S2, in all transfected cells, the transfection effect of PEI/mRNA/PAN2H group was significantly stronger than that of PEI/mRNA transfection group.

RNase Protection and Physicochemical Characterization of PEI/mRNA/PAN2H NPs

mRNA vaccines, as next-generation immunogens, offer several advantages over conventional vaccines, including potent immunogenicity, rapid production, flexible design, and broad protection potential. However, poor stability as well as low transfection efficiency in vivo limits their efficiency to elicit an effective immune response. To evaluate the stability of the constructed PEI/mRNA/PAN2H NPs, an *RNase* I protection assay was performed using naked mRNA and nanoparticle-encapsulated mRNA. As shown in Figure 4A, naked mRNA was readily degraded after *RNase* I treatment (lane 2), whereas mRNA encapsulated in PEI/mRNA/PAN2H nanoparticles remained intact after *RNase* I incubation

https://doi.org/10.2147/IJN.S514056

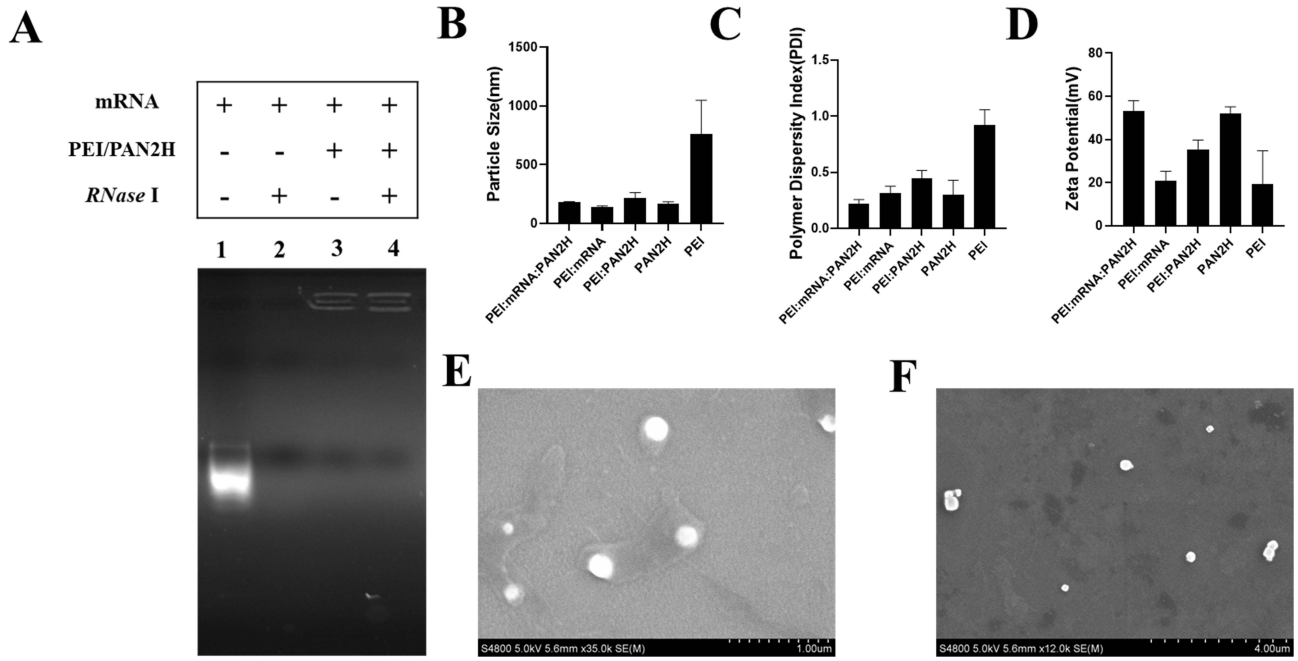

Figure 4 The characterization of PEI/mRNA/PAN2H NPs. (**A**) *RNase I* degradation assay of PEI/mRNA/PAN2H. Lane 1 is the mRNA, Lane 2 is the mRNA incubated with *RNase I*, Lane 3 is the PEI/mRNA/PAN2H, Lane 4 is the PEI/mRNA/PAN2H digested with *RNase I*; (**B**) The partial size of PAN2H, PEI/mRNA, PEI/PAN2H, PEI/mRNA/PAN2H; (**C**) The PDI of PAN2H, PEI/mRNA, PEI/PAN2H, PEI/mRNA/PAN2H; (**D**) The zeta potential of PAN2H, PEI/mRNA, PEI/PAN2H, PEI/mRNA/PAN2H; (**E**) The morphological results of PEI/mRNA; (**F**) The morphological results of PEI/mRNA/PAN2H.

(lane 4). Taken together, these results indicate that PEI/mRNA/PAN2H NPs are able to resist *RNase I* degradation after encapsulation of mRNA.

The optimized PEI/mRNA/PAN2H was formulated according to the above optimal ratio, and the morphology of PAN2H and PEI/mRNA/PAN2H was observed by scanning electron microscopy. As shown in Figure 4E and F, the PAN2H and PEI/mRNA/PAN2H showed a spherical morphology with a smooth surface and more homogeneous particle size. Quantitative analysis revealed that the nanocomplexes formed compact structures with an average diameter of 183.8 nm (Figure 4B) and a narrow size distribution (Figure 4C), indicating high homogeneity. Furthermore, the nanoparticles exhibited a highly positive surface charge with an average zeta potential of 53 mV (Figure 4D), a property known to facilitate interaction with anionic cell membranes. Overall, the results show that the PAN2H and PEI/PAN2H bind to mRNA through electrostatic interaction and can effectively compress mRNA to form nanoparticles, thereby reducing particle size while increasing surface charge.

In vivo Safety Assessment of the PEI/mRNA/PAN2H NPs

To evaluate the in vivo safety of the mRNA delivery system, PBS, PEI, PAN2H, PEI/RBD (containing 30 μg RBD mRNA), PEI/S1 (containing 30 μg S1 mRNA), PEI/RBD/PAN2H (containing 30 μg RBD mRNA), and PEI/S1/PAN2H (containing 30 μg S1 mRNA) were prepared and immunized in vivo. There were no undesirable changes in the vaccine injection sites, and no obvious differences were found in the body weights of mice in all immunized groups (Figure 5A). At day 28 after the prime immunization, the spleen, lung, heart, liver, and kidney tissues of the control group and each test group were sectioned and observed, and the results of H&E staining showed that the tissues of each group had normal morphology and structure, no inflammatory cell infiltration, no obvious petechial hemorrhage and inflammatory exudate, which indicated that the PEI/mRNA and PEI/mRNA/PAN2H NPs fabricated did not produce observable acute histopathological abnormalities under the tested conditions and demonstrated acceptable short-term biocompatibility for nucleic acid delivery (Figure 5B).

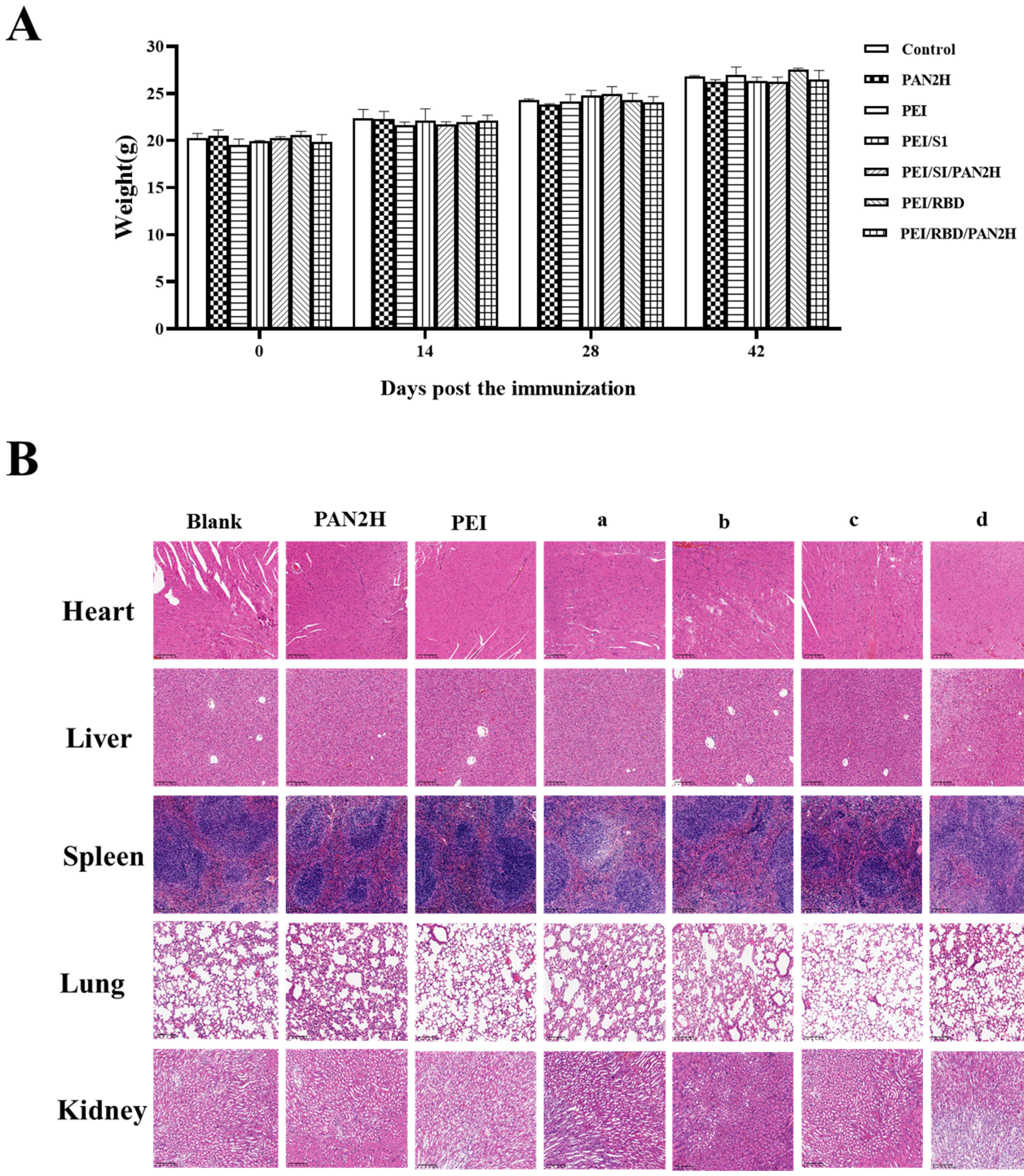

Figure 5 In vivo safety assessment of the PEI/mRNA/PAN2H NPs. BALB/c mice received an intramuscular injection of PBS, PAN2H, PEI, PEI/S1, PEI/S1/PAN2H, PEI/RBD, and PEI/RBD/PAN2H. (**A**) The body weight changes of BALB/c mice after immunization; (**B**) H&E staining of major organs collected from mice in the PBS, PAN2H, PEI, PEI/S1 (a), PEI/S1/PAN2H (b), PEI/RBD (c), and PEI/RBD/PAN2H (d) groups.

Measurement of Changes in IgG Antibodies After Immunization

To confirm that PEI/mRNA/PAN2H nanoparticles could mediate the intracellular expression of PEDV antigens, HEK-293T cells were transfected with S1- or RBD-encoding mRNA formulations, and antigen expression was verified by indirect immunofluorescence. In the indirect immunofluorescence assay (Figure S3), green fluorescence was observed in

https://doi.org/10.2147/IJN.S514056

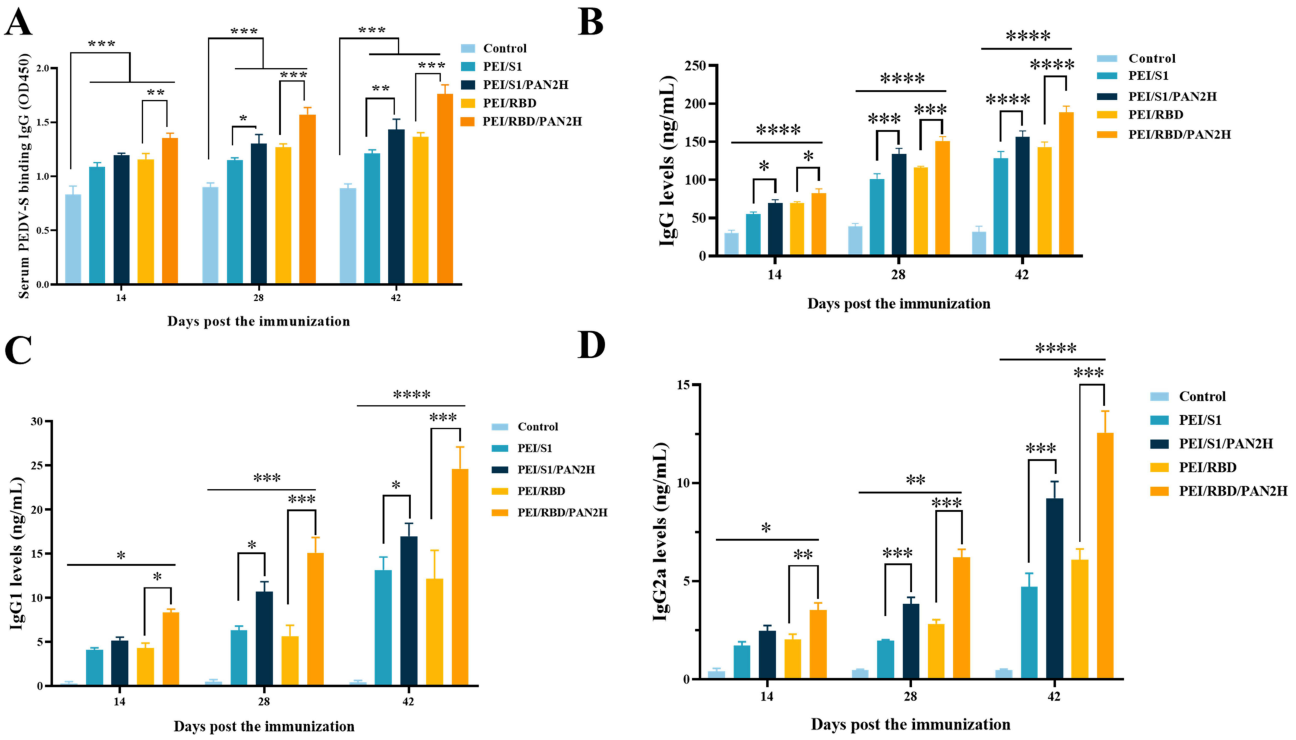

Figure 6 Evaluation of in vivo immunization effect of the PEI/mRNA/PAN2H NPs. (**A**) Measurement of changes in specific IgG antibodies after immunization; (**B**) Measurement of changes in total IgG antibodies after immunization; (**C**) Measurement of changes in total IgG1 antibodies after immunization; (**D**) Measurement of changes in total IgG2a antibodies after immunization. Data are presented as mean ± SD (biological replicates, n = 3 mice per group analyzed; total group size = 6 mice per group). Statistical significance: *$p < 0.05$, **$p < 0.01$, ***$p < 0.001$, ****$p < 0.0001$.

the cytoplasm. These results indicate that PEI/PAN2H NPs can effectively encapsulate the mRNA vaccine and transfect cells to express the proteins, suggesting that they can be used for vaccine delivery.

To further validate whether the PEI/mRNA/PAN2H NPs could be used for mRNA vaccine delivery and induce enhanced immune responses. We performed in vivo immunization experiments and measured the levels of specific PEDV IgG (Figure 6A), total IgG (Figure 6B), total IgG1 (Figure 6C) and total IgG2a (Figure 6D) antibodies in serum samples by ELISA on days 14, 28 and 42 post the first immunization. At days 14, 28 and 42 post the first immunization, the levels of total IgG, IgG1 and IgG2a were significantly higher in the PEI/RBD/PAN2H Group and the PEI/S1/PAN2H Group than those in the PEI/RBD Group and the PEI/S1 Group, which confirmed the transfection efficiency of the PEI/PAN2H. These results indicate that PAN2H incorporation enhanced the in vivo immunogenicity of the PEI-based delivery system. To further assess Th1/Th2 skewing, the IgG2a/IgG1 ratios were calculated from the same dataset (n = 3). The IgG2a/IgG1 ratios were comparable among groups at Days 14, 28, and 42, with no significant inter-group differences at each time point (Figure S4). Therefore, under the present study design, the data support a relatively balanced Th1/Th2-associated antibody response rather than a clearly polarized immune bias. In conclusion, the transfection ability of PEI/PAN2H was significantly enhanced in vivo and in vitro compared with that of PEI.

Measurement of Cytokine Changes and Splenocyte Proliferation After Immunization

Humoral immunity usually provides protection only against specific subtypes of viral strains, whereas cellular immunity provides protection against different subtypes of viral infections; for example, several human studies have reported that coronavirus-specific CD8+ and CD4+ T cells contribute to protective immunity. We investigated the potential mechanism by which PEI/PAN2H NPs induce higher antibodies than PEI. As shown in Figure 7A and B, the serum levels of IL-4 (Figure 7A) and IFN-γ (Figure 7B) were significantly higher in the PEI/mRNA/PAN2H NPs group than in the PEI/mRNA immunized group. These findings suggest that incorporation of PAN2H enhances systemic immune activation

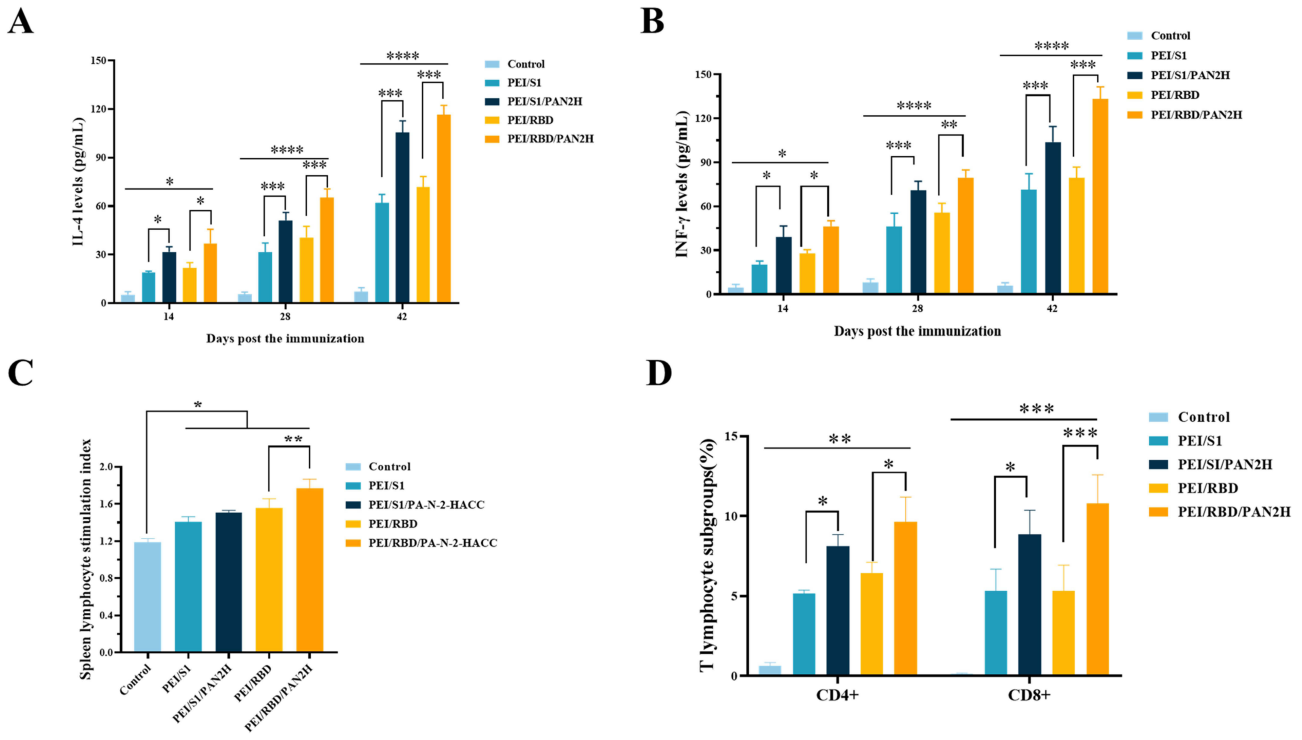

Figure 7 Serum cytokine levels, splenocyte proliferation, and T-cell subpopulations after vaccination. (**A** and **B**) The levels of cytokine IL-4 (**A**) and IFN-γ (**B**) of each group in immunized mice. (**C**) The lymphocyte proliferative response of each group after immunization; (**D**) The changes of spleen CD4+ and CD8+ T lymphocytes of each group after immunization. Data are presented as mean ± SD (biological replicates, n = 3 mice per group analyzed; total group size = 6 mice per group). Statistical significance: *$p < 0.05$, **$p < 0.01$, ***$p < 0.001$, ****$p < 0.0001$.

under the present experimental conditions. The serum cytokine measurements reported here reflect overall immune response trends in vivo.

The proliferation of splenic lymphocytes in PEI/mRNA/PAN2H NPs intramuscularly-immunized mice showed more proliferation than that in PEI/mRNA group and the PBS group (P<0.01) (Figure 7C). These results suggest that muscle immunization with PEI/mRNA/PAN2H NPs produces a superior lymphocyte proliferative response. CD4+ T lymphocytes are helper T lymphocytes, whose main role is to enhance phagocyte-mediated anti-infective effects as well as to enhance B-cell-mediated humoral immune response, while CD8+ T lymphocytes are killer T lymphocytes, whose main role is to specifically kill target cells. Splenocytes were isolated 5 weeks after the first immunization, and T-lymphocyte subpopulations were assayed by using flow cytometry. Compared with the PEI/mRNA and the control group, the PEI/mRNA/PAN2H groups showed higher proportions of $CD4^+$ and $CD8^+$ T lymphocytes (Figures 7D and S5). This suggests that PEI/mRNA/PAN2H intramuscular immunization induces more cytokines, which leads to stronger cellular immune responses.

Discussion

In this study, we demonstrated that the PEI/mRNA/PAN2H platform can effectively enhance the transfection efficiency and immunization efficacy of mRNA vaccines in vitro and in vivo. We showed that mRNA complexed with the PEI/mRNA/PAN2H can efficiently achieve eGFP- and Fluc-mRNA expression in transduced HEK-293T cells, with stronger expression than that achieved by the commercial transfection agents tested. We further demonstrated that PEI/mRNA/PAN2H effectively delivered mRNA in vivo and induced stronger levels of humoral and cellular immunity compared to PEI controls. In addition, the addition of PEI/mRNA/PAN2H in vivo and in vitro did not lead to significant toxicity. Taken together, these findings support PEI/mRNA/PAN2H as a promising non-lipid delivery platform for mRNA expression and vaccine immunoenhancement. These are encouraging novel findings from the perspective of PEI/MRNA/PAN2H as a potential delivery platform.

https://doi.org/10.2147/IJN.S514056

As immunogens for next-generation vaccines, mRNA vaccines have many advantages compared with traditional vaccines, such as high immunogenicity, easy and fast production, rapid development of novel vaccines, easy updating and broad protection.[1,2] However, poor stability as well as low transfection efficiency in vivo limit their efficiency to elicit an effective immune response.[2,31,37–40] To solve these problems, several methods have been developed.[41] PEI is a synthetic polymer that compresses siRNA and DNA into a complex that is efficiently absorbed by cells for gene therapy.[17] To enhance the transfection effect of PEI, some studies have attached PEI to the surface of nanoparticles by covalent and electrostatic means, which can effectively promote the delivery of mRNA.[42] Chitosan-based nanoparticles are biodegradable nanoparticles that possess the role of delivering antigens and immune enhancers, and their safety and efficacy have been widely validated. In this study, PAN2H NPs were selected as nanoparticles and combined with PEI to prepare a novel delivery platform. The average diameter of PEI/mRNA/PAN2H was 183.8 nm, with a zeta potential of 53 mV, which may facilitate cellular association in vitro. However, such a highly positive surface charge may also promote nonspecific protein adsorption and protein corona formation in biological fluids, potentially affecting colloidal stability, cellular specificity, and in vivo biodistribution. To further evaluate colloidal behavior under biologically relevant conditions, we characterized particle size and ζ-potential in the presence of serum. Under serum-containing conditions, PEI/mRNA/PAN2H complexes showed an increase in hydrodynamic diameter compared with PEI/mRNA complexes, but remained colloidally stable and retained a net positive surface charge that was higher than that of the PEI/mRNA group (Figure S6). This maintained positive surface character in serum may partially contribute to the enhanced transfection observed under serum-containing conditions. The electrostatic adsorption of PEI/PAN2H binds to negatively charged mRNAs, which can effectively protect the mRNA from the degradation of *RNase I*, and improve the stability and transfection efficiency of mRNA.

PEIs or cationic particles can efficiently transport nucleic acid cargoes into the cytosol, the high cationic charge density and strong proton-buffering behavior of PEI are major contributors to its cytotoxicity. Currently, there are several experiments to reduce the toxicity of PEIs, including neutralization of cationic charge with anhydride, different ketonization, alteration of PEI cross-linking by adjusting the disulfide bonding content, and the use of shorter polymers.[17,20–22,26] In this study, we found that the addition of PAN2H significantly increased the expression of eGFP and Fluc mRNA in cells compared to the PEI/mRNA transfected group. The in vivo immunization results confirmed that PEI/MRNA/PAN2H efficiently delivered mRNA in vivo and induced stronger levels of humoral and cellular immunity compared to PEI control. These findings suggest that incorporation of PAN2H may help reduce the PEI burden required to achieve effective delivery, although this will require formal dose-optimization studies.

PEDV is one of the major causes of piglet mortality and a safe and effective vaccine is of great importance. The RBD region of S protein has been reported to contain neutralizing epitopes and potential co-receptor binding regions of PEDV and is widely used as the antigen for PEDV vaccine development.[30,31] In this study, two mRNA vaccines encoding S1 or RBD proteins were prepared, and the immunogenicity was investigated in mice. The result showed that the PEI/RBD/PAN2H mRNA vaccine could induce more antibodies than the PEI/S1/PAN2H mRNA vaccine. In addition, humoral immunity usually provides protection only against specific subtypes of viral strains, whereas cellular immunity provides protection against different subtypes of viral infections; for example, several human studies have reported that coronavirus-specific CD8+ and CD4+ T cells contribute to protective immunity.[43,44] In this study, we found that PEI/mRNA/PAN2H immunized group induced more serum IFN-γ and IL-4 cytokines than PEI/PEDV mRNA group ($p<0.05$); and the results of flow cytometry analysis of the T lymphocyte subsets showed that the PEI/PEDV mRNA/PAN2H group had significantly more CD4+ and CD8+ T lymphocytes were higher than the PEI/PEDV mRNA Group ($p<0.05$) indicating that the PEI/mRNA/PAN2H could induce higher humoral immune response and cellular immune response responses compared to PEI/mRNA group. To further evaluate potential Th1/Th2 immune polarization, we calculated the IgG2a/IgG1 ratio based on the subclass ELISA data. The IgG2a/IgG1 ratios did not differ significantly among immunized groups at each time point (one-way ANOVA, $p>0.05$), suggesting that PAN2H incorporation enhanced overall antibody magnitude without markedly altering Th1/Th2 bias under the present conditions. Collectively, these findings support improved immunogenic performance of the PAN2H-containing formulation in the mouse model used in this study.

Conclusions

We have developed a potential mRNA delivery system that exhibits resistance to *RNase* degradation, high transfection efficiency, and enhanced immunogenicity compared with the PEI/mRNA group. Immunization with PEI/mRNA/PAN2H NPs induced higher levels of specific antibodies and cellular immune responses without the use of any adjuvant. While the enhanced immune responses observed here are encouraging, assessment of long-term immune durability and protective efficacy in target-species challenge models will further define its translational potential. Overall, these findings provide proof-of-concept evidence that PEI/mRNA/PAN2H is a promising non-lipid mRNA delivery platform.

Data Sharing Statement

All materials and data used in this research are accessible in the manuscript and its Supplementary Information files. All relevant data are available from the corresponding author upon request.

Author Contributions

All authors made a significant contribution to the work reported, whether that is in the conception, study design, execution, acquisition of data, analysis and interpretation, or in all these areas; took part in drafting, revising or critically reviewing the article; gave final approval of the version to be published; have agreed on the journal to which the article has been submitted; and agree to be accountable for all aspects of the work.

Funding

This work was supported by the National Natural Science Foundation of China (32370987), National Key R&D Program of China (Intergovernmental International Scientific and Technological Innovation Cooperation Key Special Program, China–Malaysia Young Scientists Exchange Program; SQ2025YFE0109155), Key Project of Zhejiang Provincial Natural Science Foundation of China (LZ26C180002), Sichuan Science and Technology Program (2026YFHZ0150) and Agricultural Science and Technology Program in Taizhou (24nya05, 202410, 25nya07, 25nya17 and 25nya05).

Disclosure

The authors declare no competing interest in this work.

References

1. Gebre MS, Brito LA, Tostanoski LH, Edwards DK, Carfi A, Barouch DH. Novel approaches for vaccine development. *Cell*. 2021;184(6):1589–1603. doi:10.1016/j.cell.2021.02.030
2. Baden LR, Sahly HME, Essink B, et al. Efficacy and safety of the mRNA-1273 SARS-CoV-2 vaccine. *N Engl J Med*. 2021;384(5):403–416. doi:10.1056/NEJMoa2035389
3. Hassett KJ, Higgins J, Woods A, et al. Impact of lipid nanoparticle size on mRNA vaccine immunogenicity. *J Control Release*. 2021;335:237–246. doi:10.1016/j.jconrel.2021.05.021
4. Li X, Xing R, Xu C, et al. Immunostimulatory effect of chitosan and quaternary chitosan: a review of potential vaccine adjuvants. *Carbohydr Polym*. 2021;264:118050. doi:10.1016/j.carbpol.2021.118050
5. Jin Z, Li W, Cao H, Zhang X, Zhao K. Antimicrobial activity and cytotoxicity of N-2-HACC and characterization of nanoparticles with N-2-HACC and CMC as a vaccine carrier. *Chem Eng J*. 2013;221:331–341. doi:10.1016/j.cej.2013.02.011
6. Qin Z, Nai Z, Li G, et al. The oral inactivated porcine epidemic diarrhea virus presenting in the intestine induces mucosal immunity in mice with alginate-chitosan microcapsules. *Animals*. 2023;13(5). doi:10.3390/ani13050889
7. Deng K, Huang Z, Jing B, et al. Mucoadhesive chitosan-catechol as an efficient vaccine delivery system for intranasal immunization. *Int J Biol Macromol*. 2024;273:133008. doi:10.1016/j.ijbiomac.2024.133008
8. Shao C, Yu Z, Luo T, et al. Chitosan-coated selenium nanoparticles attenuate PRRSV replication and ROS/JNK-Mediated apoptosis *in vitro*. *Int J Nanomed*. 2022;17:3043–3054. doi:10.2147/IJN.S370585
9. Mokhtar H, Biffar L, Somavarapu S, et al. Evaluation of hydrophobic chitosan-based particulate formulations of porcine reproductive and respiratory syndrome virus vaccine candidate T cell antigens. *Vet Microbiol*. 2017;209:66–74. doi:10.1016/j.vetmic.2017.01.037
10. Chen Y, Song T, Xiao Y-L, et al. Enhancement of immune response of piglets to PCV-2 vaccine by porcine IL-2 and fusion IL-4/6 gene entrapped in chitosan nanoparticles. *Res Veter Sci*. 2018;117:224–232. doi:10.1016/j.rvsc.2017.12.004
11. Zhao K, Zhang Y, Zhang X, et al. Preparation and efficacy of Newcastle disease virus DNA vaccine encapsulated in chitosan nanoparticles. *Int J Nanomed*. 2014;9:389–402. doi:10.2147/IJN.S54226
12. Lampe AT, Farris EJ, Brown DM, Pannier AK. High- and low-molecular-weight chitosan act as adjuvants during single-dose influenza A virus protein vaccination through distinct mechanisms. *Biotechnol Bioeng*. 2021;118(3):1224–1243. doi:10.1002/bit.27647

13. Moghadam NA, Bagheri F, Eslaminejad MB. Chondroitin sulfate modified chitosan nanoparticles as an efficient and targeted gene delivery vehicle to chondrocytes. *Colloids Surf B Biointerfaces*. 2022;219:112786. doi:10.1016/j.colsurfb.2022.112786
14. Gholap AD, Kapare HS, Pagar S, et al. Exploring modified chitosan-based gene delivery technologies for therapeutic advancements. *Int J Biol Macromol*. 2024;260(Pt 2):129581. doi:10.1016/j.ijbiomac.2024.129581
15. Cui K, Fangming Z, Shi T, et al. Iterative screening of vitamin E-based functional lipid nanoparticles for mRNA delivery. *ACS Nano*. 2025;19 (22):20672–20692. doi:10.1021/acsnano.5c01378
16. Wang H, Liu X, Ai X, et al. Safe and effective delivery of mRNA using modified PEI-based lipopolymers. *Pharmaceutics*. 2023;15(2). doi:10.3390/pharmaceutics15020410
17. Casper J, Schenk SH, Parhizkar E, Detampel P, Dehshahri A, Huwyler J. Polyethylenimine (PEI) in gene therapy: current status and clinical applications. *J Control Release*. 2023;362:667–691. doi:10.1016/j.jconrel.2023.09.001
18. Ochrimenko S, Vollrath A, Tauhardt L, et al. Dextran-graft-linear poly(ethylene imine)s for gene delivery: importance of the linking strategy. *Carbohydr Polym*. 2014;113:597–606. doi:10.1016/j.carbpol.2014.07.048
19. Zhang X, Duan Y, Wang D, Bian F. Preparation of arginine modified PEI-conjugated chitosan copolymer for DNA delivery. *Carbohydr Polym*. 2015;122:53–59. doi:10.1016/j.carbpol.2014.12.054
20. Tripathi SK, Goyal R, Kashyap MP, et al. Depolymerized chitosans functionalized with bPEI as carriers of nucleic acids and tuftsin-tethered conjugate for macrophage targeting. *Biomaterials*. 2012;33(16):4204–4219. doi:10.1016/j.biomaterials.2012.02.035
21. Nam J-P, Nah J-W. Target gene delivery from targeting ligand conjugated chitosan–PEI copolymer for cancer therapy. *Carbohydr Polym*. 2016;135:153–161. doi:10.1016/j.carbpol.2015.08.053
22. Yamada H, Loretz B, Lehr C-M. Design of starch-graft-PEI polymers: an effective and biodegradable gene delivery platform. *Biomacromolecules*. 2014;15(5):1753–1761. doi:10.1021/bm500128k
23. Cui L, Cohen JL, Chu CK, Wich PR, Kierstead PH, Frechet JM. Conjugation chemistry through acetals toward a dextran-based delivery system for controlled release of siRNA. *J Am Chem Soc*. 2012;134(38):15840. doi:10.1021/ja305552u
24. Ren J, Cao Y, Li L, et al. Self-assembled polymeric micelle as a novel mRNA delivery carrier. *J Control Release*. 2021;338:537–547. doi:10.1016/j.jconrel.2021.08.061
25. Dong S, Feng Z, Ma R, et al. Engineered design of a mesoporous silica nanoparticle-based nanocarrier for efficient mRNA delivery *in vivo*. *Nano Lett*. 2023;23(6):2137–2147. doi:10.1021/acs.nanolett.2c04486
26. Taranejoo S, Chandrasekaran R, Cheng W, Hourigan K. Bioreducible PEI-functionalized glycol chitosan: a novel gene vector with reduced cytotoxicity and improved transfection efficiency. *Carbohydr Polym*. 2016;153:160–168. doi:10.1016/j.carbpol.2016.07.080
27. Thakur S, Saini RV, Thakur N, et al. Chitosan-PEI passivated carbon dots for plasmid DNA and miRNA-153 delivery in cancer cells. *Heliyon*. 2023;9(11):e21824. doi:10.1016/j.heliyon.2023.e21824
28. Li M, Pan Y, Xi Y, Wang M, Zeng Q. Insights and progress on epidemic characteristics, genotyping, and preventive measures of PEDV in China: a review. *Microb Pathog*. 2023;181:106185. doi:10.1016/j.micpath.2023.106185
29. Zhang H, Zou C, Peng O, et al. Global dynamics of porcine enteric coronavirus PEDV epidemiology, evolution, and transmission. *Mol Biol Evol*. 2023;40(3). doi:10.1093/molbev/msad052
30. Wen Z, Xu Z, Zhou Q, et al. Oral administration of coated PEDV-loaded microspheres elicited PEDV-specific immunity in weaned piglets. *Vaccine*. 2018;36(45):6803–6809. doi:10.1016/j.vaccine.2018.09.014
31. Zhao Y, Fan B, Song X, et al. PEDV-spike-protein-expressing mRNA vaccine protects piglets against PEDV challenge. *mBio*. 2024;15(2): e0295823. doi:10.1128/mbio.02958-23
32. Thavorasak T, Chulanetra M, Glab-Ampai K, et al. Novel neutralizing epitope of PEDV S1 protein identified by IgM monoclonal antibody. *Viruses*. 2022;14(1). doi:10.3390/v14010125
33. Eker Fidan EB, Bal K, Şentürk S, Kaplan Ö, Demir K, Gök MK. Enhancing gene delivery efficiency with amphiphilic chitosan modified by myristic acid and tertiary amino groups. *Int J Biol Macromol*. 2024;282(Pt 1):136775. doi:10.1016/j.ijbiomac.2024.136775
34. Sharma D, Singh J. Synthesis and characterization of fatty acid grafted chitosan polymer and their nanomicelles for nonviral gene delivery applications. *Bioconjug Chem*. 2017;28(11):2772–2783. doi:10.1021/acs.bioconjchem.7b00505
35. Xie Y, Jin Z, Ma D, Yin TH, Zhao K. Palmitic acid- and cysteine-functionalized nanoparticles overcome mucus and epithelial barrier for oral delivery of drug. *Bioeng Transl Med*. 2023;8(3):e10510. doi:10.1002/btm2.10510
36. Zhao K, Rong G, Teng Q, et al. Dendrigraft poly-L-lysines delivery of DNA vaccine effectively enhances the immunogenic responses against H9N2 avian influenza virus infection in chickens. *Nanomedicine*. 2020;27:102209. doi:10.1016/j.nano.2020.102209
37. Bitounis D, Jacquinet E, Rogers MA, Amiji MM. Strategies to reduce the risks of mRNA drug and vaccine toxicity. *Nat Rev Drug Discov*. 2024;23 (4):281–300. doi:10.1038/s41573-023-00859-3
38. Fang Z, Yu P, Zhu W. Development of mRNA rabies vaccines. *Hum Vaccin Immunother*. 2024;20(1):2382499. doi:10.1080/21645515.2024.2382499
39. Huang J, Hu Y, Niu Z, et al. Preclinical efficacy of cap-dependent and independent mRNA vaccines against bovine viral diarrhea virus-1. *Vet Sci*. 2024;11(8). doi:10.3390/vetsci11080373
40. Richner JM, Himansu S, Dowd KA, et al. Modified mRNA vaccines protect against zika virus infection. *Cell*. 2017;168(6):1114–1125.e1110. doi:10.1016/j.cell.2017.02.017
41. Zhang W, Jiang Y, He Y, et al. Lipid carriers for mRNA delivery. *Acta Pharm Sin B*. 2023;13(10):4105–4126. doi:10.1016/j.apsb.2022.11.026
42. Zhang X, Wang K, Zhao Z, et al. Self-adjuvanting polyguanidine nanovaccines for cancer immunotherapy. *ACS Nano*. 2024;18(9):7136–7147. doi:10.1021/acsnano.3c11637
43. Channappanavar R, Fett C, Zhao J, Meyerholz DK, Perlman S. Virus-specific memory CD8 T cells provide substantial protection from lethal severe acute respiratory syndrome coronavirus infection. *J Virol*. 2014;88(19):11034–11044. doi:10.1128/JVI.01505-14
44. Moss P. The T cell immune response against SARS-CoV-2. *Nat Immunol*. 2022;23(2):186–193. doi:10.1038/s41590-021-01122-w